scientific reports

Check for updates

OPEN

Rapid detection of drug abuse via tear analysis using surface enhanced Raman spectroscopy and machine learning

Yingbin Wang[1], Yulong Huang[2], Xiaobao Liu[2], Chishan Kang[2] & Wenjie Wu[1]✉

With the growing global challenge of drug abuse, there is an urgent need for rapid, accurate, and cost-effective drug detection methods. This study introduces an innovative approach to drug abuse screening by quickly detecting ephedrine (EPH) in tears using drop coating deposition-surface enhanced Raman spectroscopy (DCD-SERS) combined with machine learning (ML). Using ultra performance liquid chromatography-tandem mass spectrometry (UPLC-MS/MS), the average concentration of EPH in tear fluid of Sprague-Dawley (SD) rats, measured over 3 h post-injection, was 1235 ng/mL. DCD-SERS effectively identified EPH in tear samples, with distinct Raman peaks observed at 1001 cm^{-1} and 1242 cm^{-1}. To enable rapid analysis of complex SERS data, three ML algorithms—linear discriminant analysis (LDA), partial least squares discriminant analysis (PLS-DA), and random forest (RF)—were employed. These algorithms achieved over 90% accuracy in distinguishing between EPH-injected and non-injected SD rats, with area under the ROC curve (AUC) values ranging from 0.9821 to 0.9911. This approach offers significant potential for law enforcement by being easily accessible, non-invasive and ethically appropriate for examinees, while being rapid, accurate, and affordable for examiners.

Keywords Drug abuse, Ephedrine, Tear, Surface enhanced Raman spectroscopy, Machine learning

The global crisis of drug abuse has exacerbated the challenges faced by health services and law enforcement, becoming a major concern in recent years[1]. According to the United Nations Office on Drugs and Crime (UNODC), methamphetamine is the most widely produced synthetic drug worldwide[1]. It is difficult to regulate due to its simple synthesis and low production cost[2]. Methamphetamine can be synthesized by the easily obtainable precursor ephedrine (EPH), which is found in many over-the-counter cough and cold medicines[3,4]. Rapid, accurate, and affordable methods for detecting drug abuse would be of great value to law enforcement in mitigating the devastating effects of drug abuse.

For the detection and identification of drug abuse, such as EPH and methamphetamine, common biological test materials include blood, urine, saliva and hair[5,6]. Tears, as an easily accessible biofluid, has not been explored for its practicality in detecting illicit drug use. This approach is non-invasive, ethically appropriate, and easily accessible. Tear collection can be done under supervision, making it resistant to adulteration. Additionally, tear analysis is time-saving and cost-efficient, as it often does not require isolation or pretreatment steps.

Traditional screening methods like immunoassay have high thresholds of detectability, potential cross-reactions, and limited applicability[6,7]. Immunoassay is particularly unsuitable for detecting EPH or methamphetamine due to multiple drug interactions[6]. Confirmatory methods such as gas chromatography-mass spectrometry (GC-MS), liquid chromatography-tandem mass spectrometry (LC-MS/MS), etc., are commonly used, but these technologies are expensive and time-consuming, and require trained operators in laboratories[8].

One of the recent advances in identifying drug users is surface-enhanced Raman spectroscopy (SERS), a spectroscopic analysis technique for molecular fingerprinting[9–14]. SERS is fast, sensitive and nondestructive, enabling lower concentration detection and in-situ detection[9–14]. An improved variant, the drop coating deposition (DCD)-SERS method, involves depositing a microvolume of solution on a SERS substrate and performing SERS after solvent evaporation[15–17]. This technique preconcentrates and localizes the analyte substance, requiring minimal sample amounts, which facilitates trace detection via tear fluids[15–17].

[1]Department of Ophthalmology, Fujian Provincial Hospital, Fuzhou University Affiliated Provincial Hospital, 134 Dongjie Rd, Fuzhou 350001, Fujian, China. [2]Shengli Clinical Medical College, Fujian Medical University, Fuzhou, Fujian, China. ✉email: wenjie_wu@foxmail.com

Of late, the combination of tears with SERS has been extensively investigated for clinical applications, including the identification of diabetes, breast cancer, gouty arthritis, and neurodegenerative diseases[18–21]. However, its practicality for screening and identifying illicit drug users has not been explored. Tear fluid testing combined with DCD-SERS might provide a rapid, accurate, affordable and ethically appropriate analytical method for workplace or roadside drug testing.

Despite the potential, the complexity of Raman data has hindered its routine use. To address this, recent studies have focused on combining Raman spectroscopy with machine learning (ML) to achieve rapid recognition[22]. In our study, we adopted ML, the data-driven approach, to classify Raman spectral data of tears. Multivariate statistical analysis was performed using three traditional ML algorithms: linear discriminant analysis (LDA), partial least squares discriminant analysis (PLS-DA) and random forest (RF).

In this study, we demonstrate for the first time the potential of combining tear fluid testing with DCD-SERS in identifying drug abuse, through the rapid detection of EPH in the tears of Sprague-Dawley (SD) rats.

Materials and methods

Experimental materials and sample collection

Ephedrine hydrochloride injections (30 mg:1 mL) were sourced from Shenyang First Pharmaceutical Co., Ltd. Solutions of the EPH reference standards were sourced from National Institutes for Food and Drug Control of China. The SERS substrate, a silicon wafer assembled with silver nanoparticles, was obtained from Xiamen Pushi Nano Technology Co., Ltd. The morphology and structure of the SERS substrates were observed using an FEI Verios G4 UC ultra-high-resolution field emission scanning electron microscope (FE-SEM; FEI, Eindhoven, the Netherlands) (Fig. 1c). The fabrication procedure of the SERS substrates is provided in the Supplementary Information. Twelve-week-old female SD rats, weighing between 280 and 300 g, were obtained from Shanghai Slac Laboratory Animal Co., Ltd. All procedures involving animals were approved by the Institutional Animal Care and Use Committee of Fujian Provincial Hospital (IACUC-FPH-SL-20230911[0093]). This study was performed in accordance with relevant guidelines and regulations. All methods are reported in accordance with ARRIVE guidelines.

Tear fluids were collected from bilateral conjunctival sac of the SD rats using quantitative capillary pipettes (2 μL), then transferred to Eppendorf tubes by squeezing a matched rubber tip. For the experimental group, SD rats received ephedrine hydrochloride (0.08 mg per gram of body weight) via intraperitoneal injection, while the control group received an equivalent volume of normal saline. Tear fluids secreted over 3 h post-injection of each SD rat were collected intermittently and stored at − 80 °C for ultra performance liquid chromatography-tandem mass spectrometry (UPLC-MS/MS) and − 4 °C for DCD-SERS. A total of 60 experimental samples and 60 control samples from 120 SD rats were collected. The procedure is illustrated in Fig. 1a. After the procedure, the euthanasia of SD rats via carbon dioxide (CO_2) inhalation was performed to minimize pain and distress. The process involved placing the SD rat in a clean, transparent chamber that allows for observation. CO_2 was then introduced into the chamber at a controlled flow rate of 20–30% of the chamber volume per minute to ensure a gradual increase in concentration, preventing distress caused by rapid changes. The rat lost consciousness within a few minutes, followed by cessation of breathing and heartbeat. The SD rats were monitored continuously throughout the process.

To explore the detection threshold of EPH in tear fluid, 2 μL of quantitative tear fluid was mixed with 1 μL of ephedrine hydrochloride diluted to various concentrations by normal saline for simulated samples and with 1 μL of normal saline for blank samples. The concentrations of EPH in the stimulated samples were 10 parts-per-million (ppm), 25 ppm, 50 ppm, 100 ppm, 250 ppm, and 500 ppm. The procedure is illustrated in Fig. 1b. Raman data were collected from these samples using DCD-SERS. For each sample, five acquisitions were taken from random points. An average spectrum derived from these five acquisitions was used for subsequent analysis.

UPLC-MS/MS measurement

The identification and quantification of EPH in tear fluid of SD rats collected over 3 h post-injection was conducted using the external standard method on UPLC-MS/MS, following the established standards for public security of China[23]. Chromatographic separation was performed using a Waters UPLC system (Waters, Milford, USA) equipped with an AB Sciex 4000 MS/MS (SCIEX, Framingham, MA, USA). An isocratic separation was achieved on a HSS T3 column (Waters, Milford, USA) with 0.1% formic acid and acetonitrile as the mobile phase at a flow rate of 0.3 mL/min for 5 min. EPH was detected and measured utilizing positive ion electrospray ionization (ESI) in multiple reactions monitoring (MRM) mode. UPLC-MS/MS data analysis was performed using PeakView software (SCIEX, Framingham, MA, USA). Further operational details are provided in the Supplementary Information.

DCD-SERS measurement

A 0.4-microliter drop of tear fluid was deposited onto the SERS substrate followed by solvent evaporation for approximately one minute at room temperature with 40% relative humidity. Raman spectra were acquired using a Renishaw inVia Reflex Raman spectrometer, equipped with a 785 nm diode laser at 10 mW power and a 50× objective lens. The spectral range was 400–3000 cm^{-1} with a spectral resolution of 1 cm^{-1} and an acquisition time of 1 s. The raw SERS data were processed using polynomial fitting for baseline correction with LabSpec (Horiba Scientifi, Kyoto, Japan). The processed SERS spectra were analyzed using the Scikit-learn package in Python (National Institute for Research in Computer Science and Automation, Rocquencourt, France) and interpreted using LabSpec.

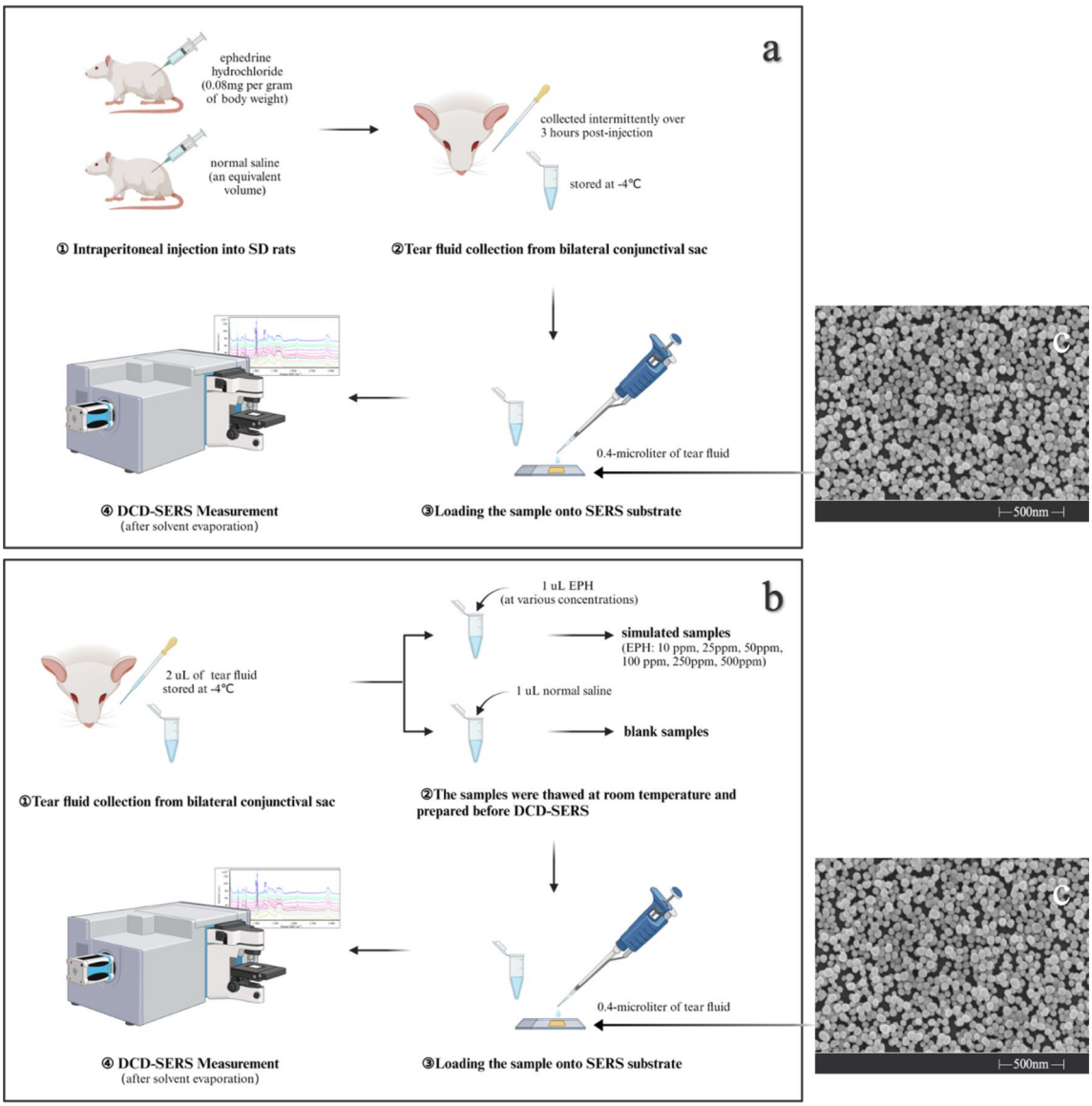

Fig. 1. Experimental procedures: experimental group and control group (**a**); simulated samples and blank samples (**b**). SEM micrograph under 200,000× magnifications of the SERS substrate (**c**).

Machine learning methods

Three traditional ML algorithms, including LDA, PLS-DA and RF, were employed to classify tear samples from SD rats with and without EPH injection, using the Sci-Kit Learn package in Python. Hyperparameter optimization for PLS-DA and RF was performed to improve classification accuracy and other performance metrics. LDA is a linear discriminant classification method that maximizes between-class variance while minimizing within-class variance to find the optimal linear boundary between different categories. PLS-DA is also a linear classification model that projects predicted and observable variables into a new space, using partial least squares regression, suitable for multivariate statistical classification. The number of latent variables was tuned to 5. RF is an ensemble learning method constructing multiple decision trees and making final decisions based on majority voting. The number of decision trees was set to 300, and the maximum depth of each decision tree was also set to 300. Monte-Carlo Cross Validation (MCCV) was used to optimize the performance of the learning algorithms. Of the 120 samples, 90 were randomly assigned to the training set and 30 to the test set. Multiple training and test dataset pairs were created by resampling the SERS data according to the same splitting ratio. Each machine learning model was trained on the training data of each pair and then applied to the corresponding test data to compute classification results. This process was repeated 100 times to verify model stability. Metrics such as accuracy, precision, recall, specificity, F1-score, and the area under the ROC curve (AUC) were calculated based on the 100 repeated trials to evaluate the strengths of the algorithms.

Results

UPLC-MS/MS analysis

The average concentration of EPH in tear fluid collected over a period of 3 h post-injection was 1235 ng/mL (1.235 ppm). The product ion spectra (MS/MS) of EPH are demonstrated in Fig. 2.

SERS spectra analysis

SERS spectra of EPH

We initially examined SERS spectra of the blank SERS substrate, a silicon wafer assembled with silver nanoparticles. Characterization of the SERS substrate by SEM are demonstrated in Fig. 1c. As shown in Fig. 3a, SERS peaks of the blank SERS substrate were found at 520, 684 and 1027 cm^{-1}. To explore the SERS peaks of EPH, as well as to evaluate the enhancement and sensitivity of the SERS substrate, EPH without dilution (30 mg:1 mL) was examined on a silicon wafer by Raman spectroscopy, and EPH at concentrations of 10 ppm, 25 ppm, 50 ppm, and 100 ppm were examined on SERS substrates by SERS (Fig. S1 in the Supplementary Information, Fig. 3b). For quantification, the enhancement factor (EF) was calculated using $EF = \frac{I_{SERS}/N_{Surf}}{I_{RS}/N_{Vol}}$ (I_{SERS}: the SERS intensity; I_{RS}: the Raman intensity; N_{Surf}: the number of adsorbed molecules; $N_{Vol} = c_{RS}V_{Sca}$ is the average number of molecules in the scattering volume (V_{Sca}) for the Raman measurement). Since the SERS substrate we used could be approximated as a single-molecule layer, the average intensity of SERS is proportional to the number (or concentration) of molecules, and this calculation can be written as $EF = \frac{I_{SERS}/c_{SERS}}{I_{RS}/c_{RS}}$ (c_{SERS}: the concentration of the analyte for SERS measurement; c_{RS}: the concentration of the analyte for Raman measurement). Based on the intensity of the peak at 1001 cm^{-1}, the EF of EPH at the SERS substrate was calculated to be approximately 10^4 (Fig. S1). In comparison with the SERS spectra of blank SERS substrate, the SERS peaks of EPH were identified at 424, 616, 752, 797, 832, 946, 1001, 1027, 1100, 1390, 1550, and 1601 cm^{-1}. Notably, as the EPH concentration decreased to 10 ppm, peaks at 1001, 1027 and 1601 cm^{-1} remained detectable.

Optimization of the spectral acquisition locations for DCD-SERS

Figure 4a is an overview of the coffee-ring formed by a dried teardrop. The coffee-ring comprises a central region which is rich in tear fern structures (Fig. 4b), and a ring region (Fig. 4c, d), illustrating the heterogenous composition of tear fluids. To optimize the spectral acquisition locations for DCD-SERS, we divided the coffee-ring into four distinct regions, labeled A, B, C, and D, corresponding to the central fern region, central blank region, inner ring region and outer ring region (Fig. 4). Ten DCD-SERS spectra were randomly collected from each region and compared accordingly (Fig. 5). To evaluate the differences in DCD-SERS signal intensities across the four regions, we employed Analysis of Variance (ANOVA) and posthoc test. ANOVA test ($P < 0.001$, F-ratio = 590.400) and posthoc test (Tukey's HSD test; $P < 0.05$) revealed significant differences between regions A-C, A-D, B-C and B-D. The central region (comprising regions A and B) showed stronger SERS signals compared to the ring regions (regions C and D). Consequently, we excluded the ring regions from SERS signal collection. For each sample, five acquisitions were taken from random points in the central region of the coffee-ring. An average spectrum derived from these five acquisitions was used for subsequent analysis.

SERS analysis of EPH in tear fluid

To explore the potential of DCD-SERS for drug abuse detection, we analyzed the spectral differences within the experimental group and control groups, as well as between the two groups. Figure 6 presents 10 representative

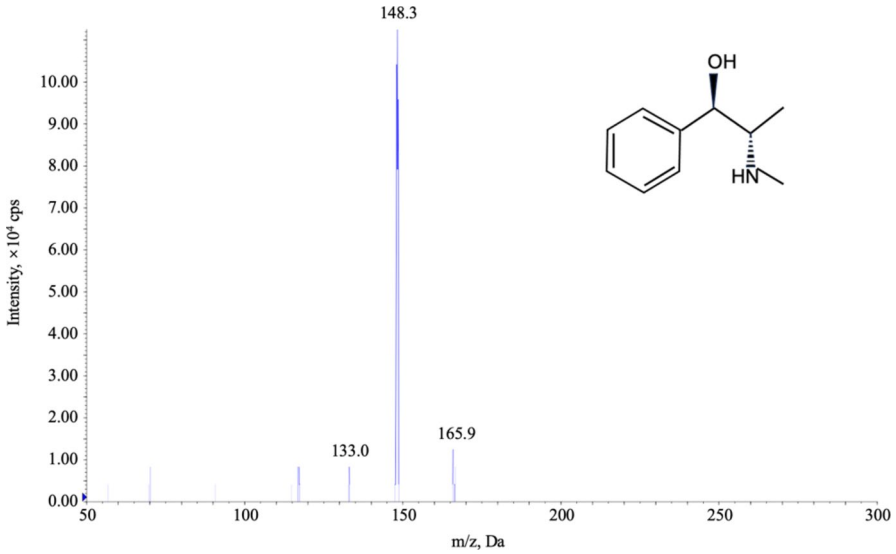

Fig. 2. Product ion spectra (MS/MS) of EPH.

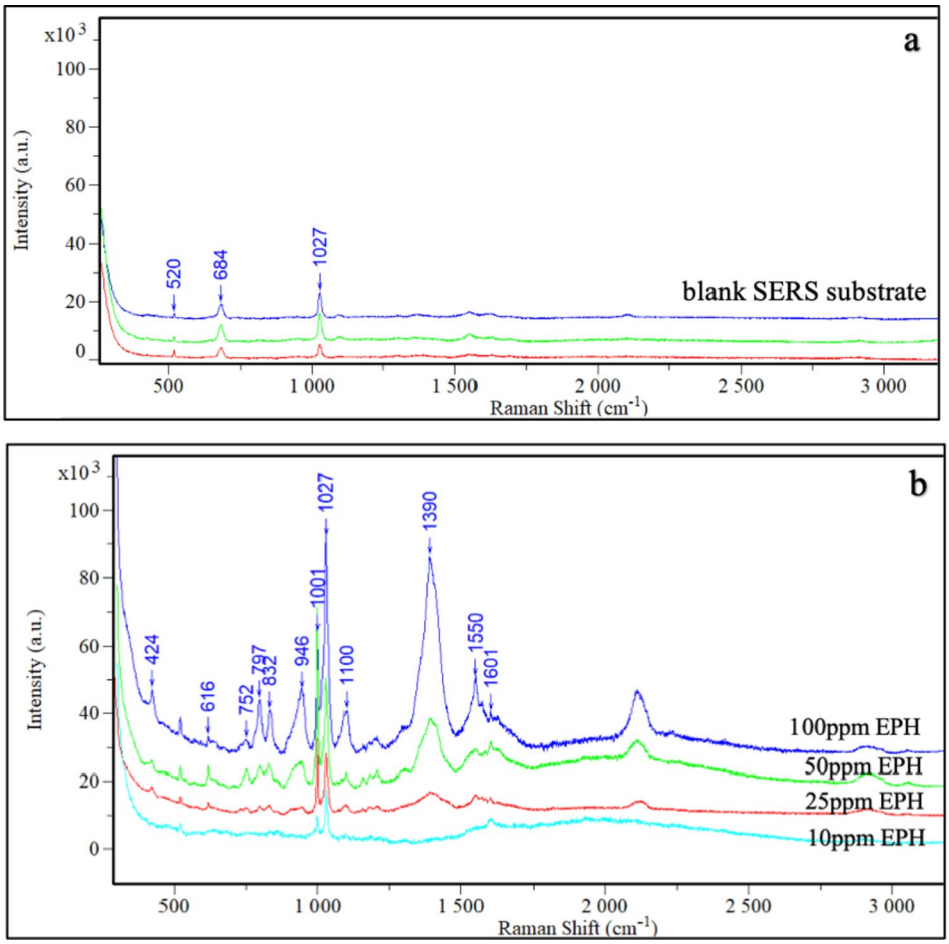

Fig. 3. SERS spectra of blank SERS substrate (**a**); SERS spectra of EPH at 10 ppm, 25 ppm, 50 ppm, and 100 ppm (**b**).

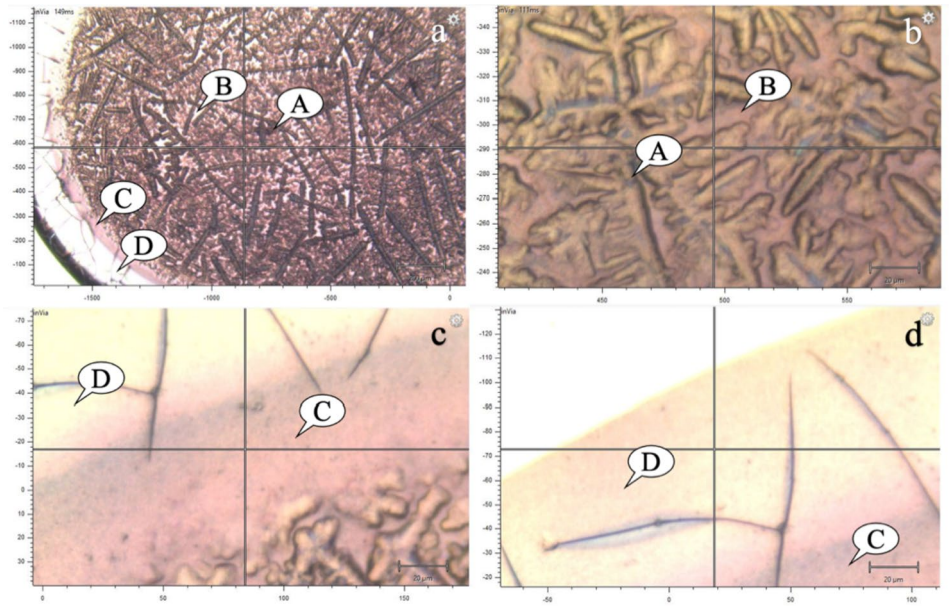

Fig. 4. (**a**) An overview of the coffee-ring formed by a dried teardrop; (**b**) a magnified view of the central region; (**c**,**d**) magnified views of the ring region. The coffee-ring pattern is divided into four distinct regions: a central fern region (A), a central blank region (B), an inner ring region (C) and an outer ring region (D).

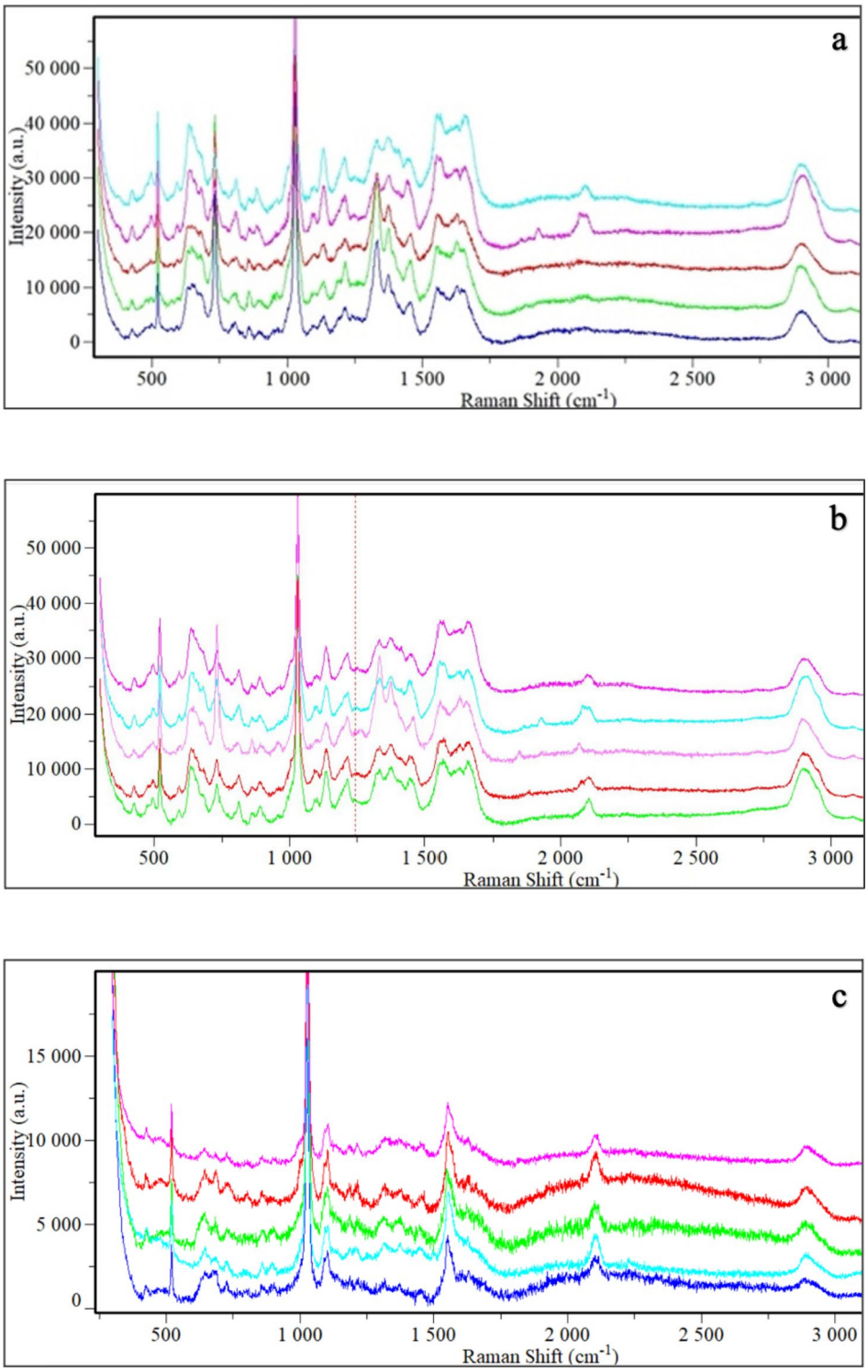

Fig. 5. DCD-SERS spectra in regions A (**a**), B (**b**), C (**c**) and D (**d**).

DCD-SERS spectra from each group. ANOVA was performed to evaluate the intra-group variation in spectral intensity, yielding p-values < 0.05, which indicate significant differences. In the experimental group, the SERS peaks of EPH at 616, 752, 797, 832, 946, 1100, 1390, 1550 and 1601 cm^{-1} were absent, while SERS peaks of EPH at 424 and 1027 cm^{-1} could be observed in both experimental and control groups (Fig. 6). Although most spectral peaks in both groups overlap, notable differences exist in peak location and intensity, particularly at 1001 cm^{-1} and 1242 cm^{-1} (Fig. 6). Independent sample *t*-test conducted on the spectral intensity at these peaks yield p values < 0.05, indicating significant differences. To further explore the detection threshold of EPH, we investigated the spectral differences between stimulated samples (with EPH concentrations at 10 ppm, 25 ppm,

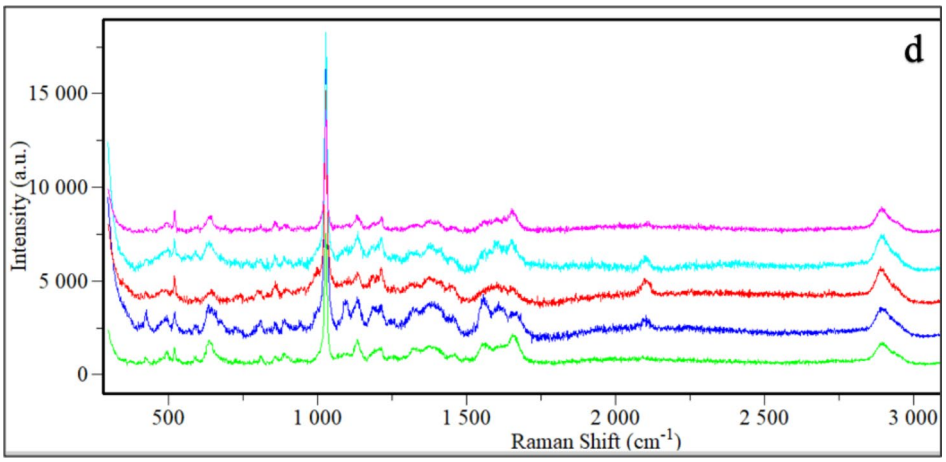

Figure 5. (continued)

50 ppm, 100 ppm, 250 ppm, and 500 ppm) and blank samples. By DCD-SERS, difference in peak intensity at 1001 cm^{-1} was observed, but not at 1242 cm^{-1}. An independent sample *t*-test on the spectral intensity at 1001 cm^{-1} between the stimulated and blank samples revealed that when the concentration of EPH was as low as 10 ppm, the p value exceeded 0.05.

Multivariate statistical analysis

The performance results, assessed using confusion matrices and receiver operating characteristic (ROC) curve analysis, are presented in Fig. 7; Table 1. Using LDA, tear samples from SD rats with or without EPH injection was classified with 93.33% accuracy, 92.86% precision, 92.86% recall, 93.75% specificity, a 92.86% F1-score and an AUC of 0.9688 after MCCV. After dimension reduction of PLS-DA, five latent variables were selected to achieve optimal performance. PLS-DA achieved 93.33% accuracy, 87.50% precision, 100.00% recall, 87.50% specificity, a 93.33% F1-score and an AUC of 0.9911 after MCCV. For RF, using 300 trees with a maximum depth of 6, the classification achieved 90.00% accuracy, 92.31% precision, 85.71% recall, 93.75% specificity, an 88.89% F1-score and an AUC value of 0.9821. The results from RF, LDA, and PLS-DA indicate that notable intra-group variability does not undermine the ability of machine learning algorithms to distinguish between groups.

Discussion

In this study, we applied DCD-SERS for the first time to detect EPH in tear fluids, highlighting its potential in drug abuse detection. Using ML, we achieved rapid differentiation between EPH-injected and non-injected SD rats.

UPLC-MS/MS analysis, a standard method for drug abuse detection, was applied to confirm that part of EPH could be excreted unchanged in tear fluids, laying a foundation for our study. The average concentration of EPH in tear fluid collected over a period of 3 h post-injection was 1235 ng/mL (1.235 ppm). The detection of EPH in tears aligns with previous studies on its excretion in other body fluids[24–26]. By comparing the Raman spectra with the SERS spectra of EPH, EF of EPH on the SERS subtrate was calculated to be approximately 10^4. We then acquired the SERS spectra of blank SERS substracts and EPH at concentrations of 10 ppm, 25 ppm, 50 ppm, and 100 ppm, finding peaks at 424, 616, 752, 832, 1001, 1027, 1601 cm^{-1} consistent with previous study[27,28]. The strongest peaks[27,28] were also at 1001 cm^{-1} and 1027 cm^{-1}. The slight differences in band positions may be due to the interaction of target analyte with the SERS substrate's nanoparticle surface. The recognition of characteristic peaks in 10 ppm EPH revealed the potential for trace EPH detection using DCD-SERS.

To optimize the spectral acquisition locations for DCD-SERS, we investigated the SERS spectral intensity across the four distinct regions of the coffee-ring. This coffee-ring pattern has been described in previous studies[29,30]. ANOVA test ($P < 0.001$, F-ratio = 590.400) and posthoc test (Tukey's HSD test; $P < 0.05$) indicated significant differences between regions A-C, A-D, B-C, B-D. The central region had stronger SERS signals compared to the ring region, differing from previous finding by S. Choi et al., likely due to the smaller teardrop volume used in our study (0.4 µL vs. 2.0 µL)[30]. We adopted smaller teardrop volume to improve user-friendliness for both the examinee and the examiner, by reducing the tear collection time and conjunctival stimulation, and accelerating the solvent evaporation process during DCD-SERS. Based on our experiment, we excluded the ring region for SERS signals collection.

To evaluate the potential of DCD-SERS for drug abuse detection, we analyzed the SERS differences of tear samples in the 400–3000 cm^{-1} range both within and between the experimental and control groups. As shown in Fig. 6, the SERS peak wavenumbers exhibit high reproducibility, demonstrating the repeatability of the measurement method. However, ANOVA test indicate significant intra-group variations in spectral intensity, which reveal the inherent heterogeneity in tear fluids among individuals. Most spectral peaks in experimental and control samples overlap, reflecting the common tear fluid components. The tentative assignments of the SERS vibrational sources, based on available SERS data from previous literature, are listed in Table 2[16,27]. In the experimental group, the SERS peaks of EPH at 616, 752, 797, 832, 946, 1100, 1390, 1550 and 1601 cm^{-1} are absent.

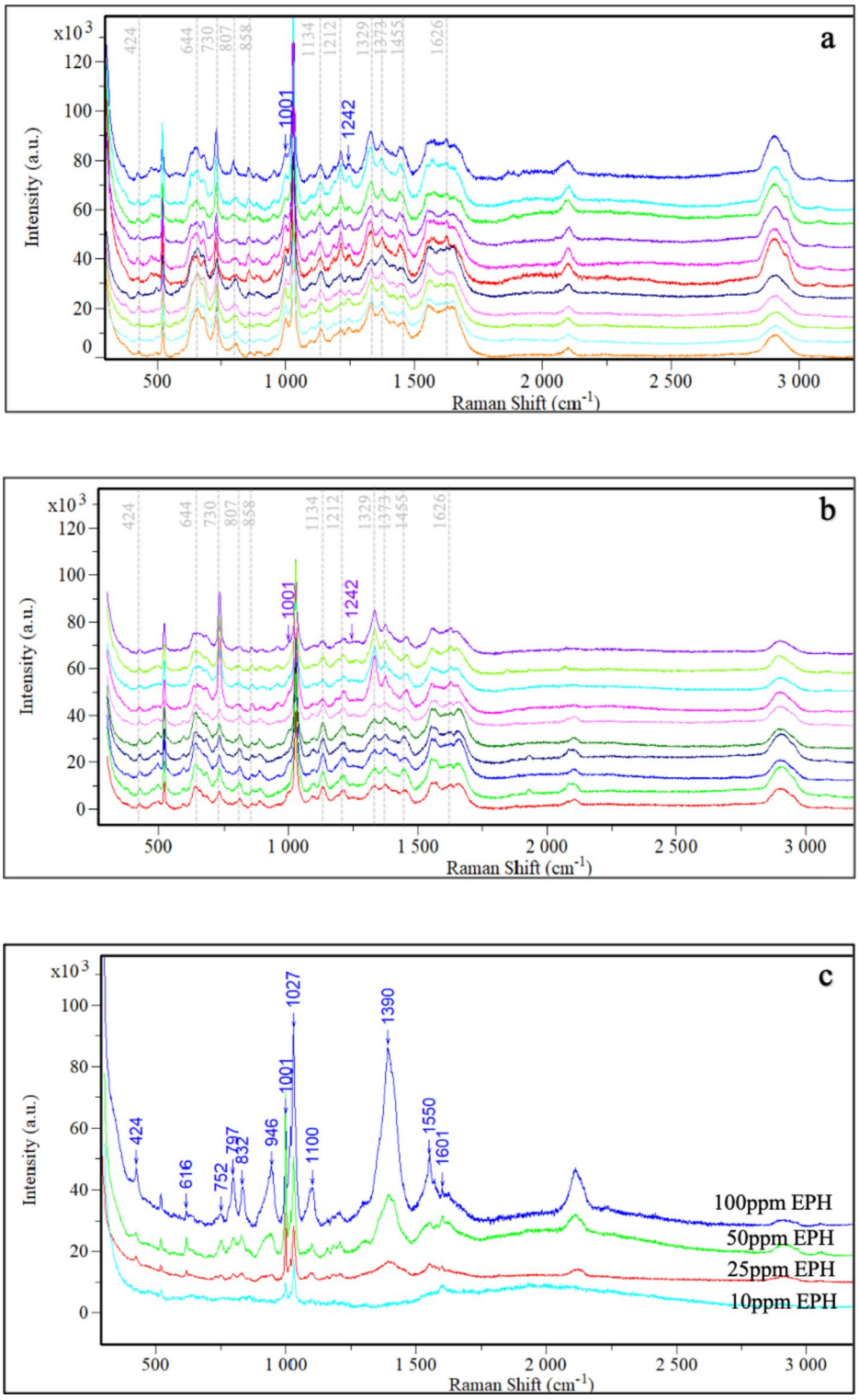

Fig. 6. (**a**) Ten representative DCD-SERS spectra of the experimental group; (**b**) Ten representative DCD-SERS spectra of the control group; (**c**) SERS spectra of EPH for reference. Notable difference in peak intensity at 1001 cm^{-1} and 1242 cm^{-1} was indicated by arrows in panel (**a**) and (**b**).

This is due to the extremely low concentration of EPH in tear fluid, which falls below the detection threshold of SERS. As shown in Fig. 3, when the concentration of EPH decreases to 10 ppm, only the Raman peaks at 1001, 1027 and 1601 cm^{-1} remain detectable, with the peak at 1001 cm^{-1} being more prominent. According to the UPLC-MS/MS quantification results, the average concentration of EPH in tear fluid collected over a period of 3 h post-injection was only 1.235 ppm. Therefore, many characteristic SERS peaks of EPH are either not

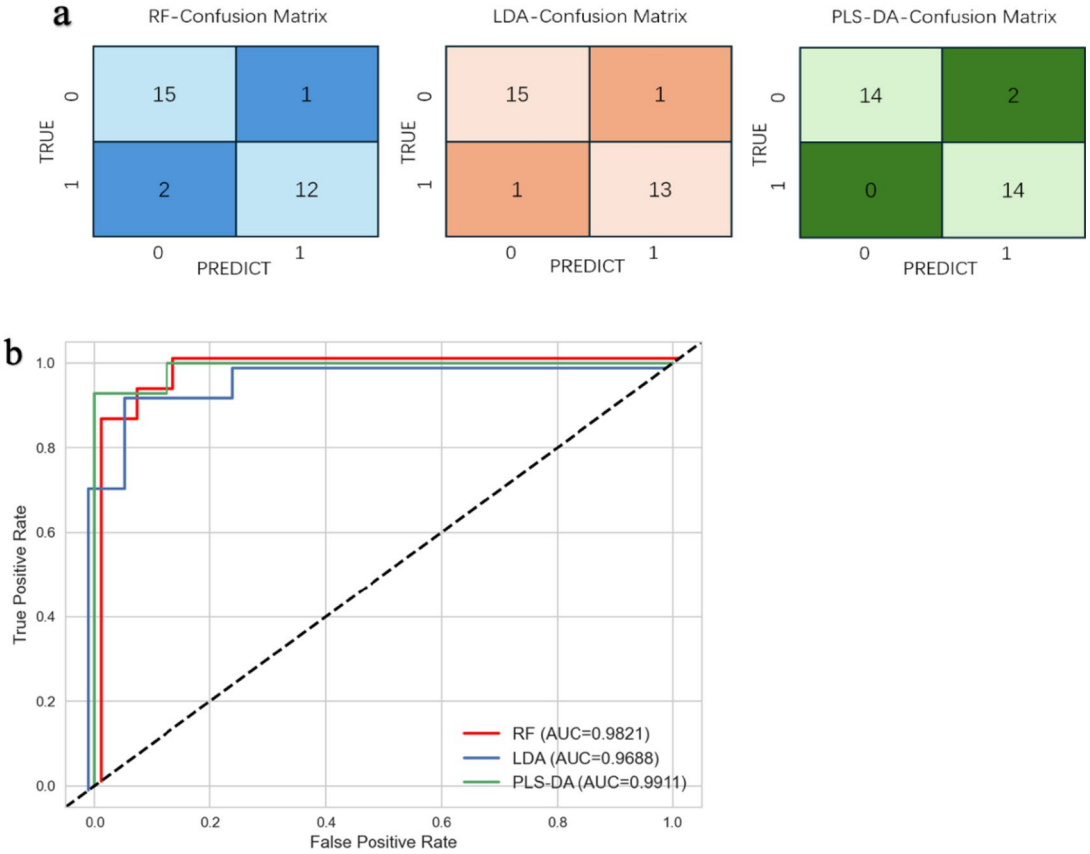

Fig. 7. Confusion matrices for the RF, LDA and PLS-DA models (**a**); ROC curves for the RF, LDA and PLS-DA models (**b**).

Method	Accuracy	Precision	Recall	Specificity	F1-score	AUC	
RF	0.9000	0.9231	0.8571	0.9375	0.8889	0.9821	
LDA	0.9333	0.9286	0.9286	0.9375	0.9286	0.9688	
PLS-DA	0.9333	0.9333	0.8750	1.0000	0.8750	0.9333	0.9911

Table 1. Multivariate statistical analysis by RF, LDA and PLS-DA. *RF* random forest, *LDA* linear discriminant analysis, *PLS-DA* partial least squares discriminant analysis.

SERS peak (cm^{-1})	Assignment	Component
424	C-C shearing, bending, and twisting	–
644	COO–wag.	Amino acids
730	COO–def.	Amino acids
807	6-ring def. C8–H wag.	DNA/RNA
858	C-C str.	Amino acids
1027	Ring breathing mode	Amino acids
1134	C8–N9 str. N9–H, C8–H bend.	DNA/RNA
1212	C5–C9 str.	DNA/RNA
1329	C-H def.	Aspartic acid, amino acids
1373	C2–H, N9–H bend. C8–N9, C4–N9 str.	DNA/RNA
1455	C–H def.	DNA/RNA, proteins, lipids and carbohydrates
1626	Indole N-H, C=O str.	Amino acids

Table 2. Principal contributions in SERS spectra of tear samples and their tentative assignments. *def.* deformation, *wag*. wagging, *str*. stretching, *bend*. bending.

visible or are obscured by the background signals of tear fluid. SERS peaks of EPH at 424 and 1027 cm^{-1} could be observed in both experimental and control groups, with the peak at 1027 cm^{-1} being more prominent. The Raman peak at 424 cm^{-1} can be assigned to the shearing, bending, and twisting vibrations of C–C bonds. The Raman peak at 1027 cm^{-1} is typically attributed to vibrational modes of the benzene ring structure, specifically C–H in-plane bending and C–C skeletal stretching vibrations[28]. Consequently, this characteristic peak may be observed in EPH, which contains a benzene ring, as well as in tear fluid, which includes amino acids and proteins. Despite the overall similarity in shape and intensity, SERS peaks at 1001 cm^{-1} and 1242 cm^{-1} can be used to distinguish between EPH-injected and non-injected SD rats. The 1001 cm^{-1} peak is directly associated with EPH, as measured previously, corresponding to the benzene ring in EPH[28]. While the 1242 cm^{-1} peak may originate from the metabolites or analogues of EPH[28].

Han et al. developed a portable kit containing SERS to detect drug abuse via urine[10]. In their study, human urine spiked with 10 ppm amphetamines underwent SERS analysis after pretreatment procedures. Several Raman peaks were attributed to amphetamines, with a strong peak at 1001 cm^{-1} suggested for high-throughput screening of drug suspects. However, identifying target analytes based solely on specific Raman peaks can be challenging. The complex signals from body fluid components often cover or overlap with those of target analyte, making the characteristic peaks of target analyte difficult to discern, especially for non-professionals. ML has been increasingly used to interpret spectral data, with many studies demonstrating its effectiveness[22]. For instance, previous researches combining dynamic-SERS and ML successfully identified methamphetamine in human urine with over 90% accuracy, though the analysis was limited to only three urine samples from three drug abusers[13,14]. While urine is the most commonly used sample, it can be easily adulterated or substituted, and spontaneous sample collection can be problematic[6]. In contrast, tear fluids offer resistance to adulteration, easy accessibility, non-invasiveness, and ethical appropriateness. To achieve rapid, accurate and efficient classification of the complex SERS data from tear fluids, our study introduced three commonly used supervised ML algorithms: LDA, PLS-DA and RF.

Generalisability is crucial when assessing ML model performance. An overfitting model struggles to handle previously unseen data in practical setting. Internal validation is widely applied for ML optimization, in which the dataset was split into training and test sets[22,31]. In the current study, MCCV, a non-exhaustive form of cross-validation, was employed. Multiple permutations of training/test dataset pairs were created by resampling the spectral data according to a predetermined splitting ratio. This process was iterated 100 times to compute the outcome. LDA achieved 93.33% accuracy, 92.86% precision, 92.86% recall, 93.75% specificity, a 92.86% F1-score, and an AUC of 0.9688 after MCCV. It provides high interpretability and computational efficiency. However, LDA assumes normal distribution and equal covariance among classes, which may not always be true. PLS-DA, which excels in handling high-dimensional data, achieved 93.33% accuracy, 87.50% precision, 100.00% recall, 87.50% specificity, a 93.33% F1-score, and an AUC of 0.9911 after MCCV. The method's ability to reduce dimensionality and handle collinear data makes it advantageous for complex datasets like Raman spectra. PLS-DA's perfect recall indicates its strength in identifying all positive cases, reducing the likelihood of false negatives. However, it had lower specificity and the risk of overfitting, especially with a small sample size. RF, a robust ensemble learning method, achieved 90.00% accuracy, 92.31% precision, 85.71% recall, 93.75% specificity, an 88.89% F1-score, and an AUC of 0.9821. It is less likely to overfit compared to PLS-DA due to its ensemble nature. RF provides robust performance with non-linear data and insights into feature importance but is computationally demanding and less interpretable. Given the potential for our technique to be used in rapid workplace or roadside drug testing, minimizing false negatives is crucial. Therefore, PLS-DA might be preferable due to its high recall and F1-score.

Conclusion

This study demonstrates that DCD-SERS can successfully detect EPH in tear fluids, with notable differences in SERS peaks at 1001 cm^{-1} (corresponding to the benzene ring in EPH) and 1242 cm^{-1}. When combined with ML, it enables rapid differentiation between EPH-injected and non-injected SD rats, demonstrating accuracy over 90% and AUC values of 0.9821–0.9911. Among RF, LDA and PLS-DA, PLS-DA might be preferable due to its high recall and F1-score. This study provides proof-of-principle for a novel approach in drug abuse screening.

Tear fluid detection via DCD-SERS addresses several limitations in conventional detection techniques of drug abuse: (a) it is easily accessible, non-invasive and ethically appropriate; (b) it can be performed under supervision; (c) it is time-saving and cost-efficient; (d) combined with a portable Raman spectrometer, it provides a quick analytical method for on-spot detection of drug abuse. Furthermore, ML enhances the ability to detect subtle patterns in the Raman spectrum, realizing the full potential of SERS. The primary limitation of our study is its preliminary nature in exploring a new approach to drug abuse screening. Future studies should focus on evaluating the limit of detection and detection time of drugs and exploring a broader range of substances, to facilitate the teanslation of this new approach into practical applications.

Data availability

The datasets generated and analysed during the current study are available from the corresponding author on reasonable request.

Received: 25 August 2024; Accepted: 3 January 2025
Published online: 07 January 2025

References

1. World Drug Report. United Nations Office on Drugs and Crime (2023). https://www.unodc.org/unodc/en/data-and-analysis/world-drug-report-2023.html

2. Winkelman, T. N. A. et al. Evaluation of amphetamine-related hospitalizations and associated clinical outcomes and costs in the United States. *JAMA Netw. Open.* **1**(6), e183758. https://doi.org/10.1001/jamanetworkopen.2018.3758 (2018).
3. Lee, J. S. et al. Analysis of the impurities in the methamphetamine synthesized by three different methods from ephedrine and pseudoephedrine. *Forensic Sci. Int.* **161**(2–3), 209–215. https://doi.org/10.1016/j.forsciint.2006.02.054 (2006).
4. Salouros, H., Collins, M., George, A. V. & Davies, S. Isolation and identification of three by-products found in methylamphetamine synthesized by the Emde route. *J. Forensic Sci.* **55**(3), 605–615. https://doi.org/10.1111/j.1556-4029.2010.01330.x (2010).
5. Vearrier, D., Curtis, J. A. & Greenberg, M. I. Biological testing for drugs of abuse. *EXS* **100**, 489–517. https://doi.org/10.1007/978-3-7643-8338-1_14 (2010).
6. Ranjkeshzadeh, H. et al. A review of drug abuse, misuse, and related laboratory challenges. *Curr. Drug Saf.* https://doi.org/10.2174/0115748863266621231023112044 (2023).
7. Mina, A. Comparison of several immunoassays used in drugs of abuse screening: Assessment against gold standard methods and calculation of measurement uncertainty. *J. Pharmacol. Toxicol. Methods* **101**, 106649. https://doi.org/10.1016/j.vascn.2019.106649 (2019).
8. Tamama, K. Advances in drugs of abuse testing. *Clin. Chim. Acta*. **514**, 40–47. https://doi.org/10.1016/j.cca.2020.12.010 (2020).
9. Shende, C., Brouillette, C. & Farquharson, S. Detection of codeine and fentanyl in saliva, blood plasma and whole blood in 5-minutes using a SERS flow-separation strip. *Analyst* **144**(18), 5449–5454. https://doi.org/10.1039/c9an01087d (2019).
10. Han, Z. et al. Portable kit for identification and detection of drugs in human urine using surface-enhanced Raman spectroscopy. *Anal. Chem.* **87**(18), 9500–9506. https://doi.org/10.1021/acs.analchem.5b02899 (2015).
11. Andreou, C., Hoonejani, M. R., Barmi, M. R., Moskovits, M. & Meinhart, C. D. Rapid detection of drugs of abuse in saliva using surface enhanced Raman spectroscopy and microfluidics. *ACS Nano*. **7**(8), 7157–7164. https://doi.org/10.1021/nn402563f (2013).
12. Sivashanmugan, K. et al. Trace detection of tetrahydrocannabinol in body fluid via surface-enhanced Raman scattering and principal component analysis. *ACS Sens.* **4**(4), 1109–1117. https://doi.org/10.1021/acssensors.9b00476 (2019).
13. Dong, R., Weng, S., Yang, L. & Liu, J. Detection and direct readout of drugs in human urine using dynamic surface-enhanced Raman spectroscopy and support vector machines. *Anal. Chem.* **87**(5), 2937–2944. https://doi.org/10.1021/acs.analchem.5b00137 (2015).
14. Weng, S. et al. Dynamic surface-enhanced Raman spectroscopy and chemometric methods for fast detection and intelligent identification of methamphetamine and 3, 4-Methylenedioxy methamphetamine in human urine. *Spectrochim Acta A* **189**, 1–7. https://doi.org/10.1016/j.saa.2017.08.004 (2017).
15. Zhang, D. et al. Raman detection of proteomic analytes. *Anal. Chem.* **75**(21), 5703–5709. https://doi.org/10.1021/ac0345087 (2003).
16. Camerlingo, C. et al. Characterization of human tear fluid by means of surface-enhanced Raman spectroscopy. *Sensors (Basel)* **19**(5). https://doi.org/10.3390/s19051177 (2019).
17. Hu, P. et al. Drop-coating deposition and surface-enhanced Raman spectroscopies (DCDRS and SERS) provide complementary information of whole human tears. *J. Raman Spectrosc.* **45**(7), 565–573. https://doi.org/10.1002/jrs.4499 (2014).
18. Cui, X. et al. Detection of glucose in diabetic tears by using gold nanoparticles and MXene composite surface-enhanced Raman scattering substrates. *Spectrochim Acta A* **266**, 120432. https://doi.org/10.1016/j.saa.2021.120432 (2021).
19. Kim, S. et al. Label-free surface-enhanced Raman spectroscopy biosensor for on-site breast cancer detection using human tears. *ACS Appl. Mater. Interfaces* **12**(7), 7897–7904. https://doi.org/10.1021/acsami.9b19421 (2020).
20. Park, M., Jung, H., Jeong, Y. & Jeong, K. H. Plasmonic Schirmer strip for human tear-based gouty arthritis diagnosis using surface-enhanced raman scattering. *ACS Nano* **11**(1), 438–443. https://doi.org/10.1021/acsnano.6b06196 (2016).
21. Cennamo, G. et al. Surface-enhanced Raman spectroscopy of tears: toward a diagnostic tool for neurodegenerative disease identification. *J. Biomed. Opt.* **25**(8), 1–12. https://doi.org/10.1117/1.JBO.25.8.087002 (2020).
22. Ralbovsky, N. M. & Lednev, I. K. Towards development of a novel universal medical diagnostic method: Raman spectroscopy and machine learning. *Chem. Soc. Rev.* **49**(20), 7428–7453. https://doi.org/10.1039/d0cs01019g (2020).
23. Hua, Z. D. et al. *Forensic Sciences: Examination Methods for Six Ephedrine Class Substances Including Norephedrine in Suspected Precurson rs, GC-MS, LC and LC-MS* (Standards Press of China, 2022).
24. Tseng, Y. L., Shieh, M. H. & Kuo, F. H. Metabolites of ephedrines in human urine after administration of a single therapeutic dose. *Forensic Sci. Int.* **157**(2–3), 149–155. https://doi.org/10.1016/j.forsciint.2005.04.008 (2006).
25. Mohamed, K. M., Al-Hazmi, A. H., Alasiri, A. M. & Ali, M. S. A GC-MS method for detection and quantification of cathine, cathinone, methcathinone and ephedrine in oral fluid. *J. Chromatogr. Sci.* **54**(8), 1271–1276. https://doi.org/10.1093/chromsci/bmw082 (2016).
26. Strano-Rossi, S., Colamonici, C. & Botrè, F. Parallel analysis of stimulants in saliva and urine by gas chromatography/mass spectrometry: perspectives for in competition anti-doping analysis. *Anal. Chim. Acta* **606**(2), 217–222. https://doi.org/10.1016/j.aca.2007.10.053 (2007).
27. Shu, T. M., Yang, X., Li, W. B. & Yao, X. J. Raman spectroscopic differences between ephedrine and pseudoephedrine. *J. Forensic Sci.* **64**(5), 1482–1485. https://doi.org/10.1111/1556-4029.14015 (2019).
28. Lv, D. et al. Rapid on-site detection of ephedrine and its analogues used as adulterants in slimming dietary supplements by TLC-SERS. *Anal. Bioanal. Chem.* **407**(5), 1313–1325. https://doi.org/10.1007/s00216-014-8380-9 (2014).
29. Capaccio, A., Sasso, A. & Rusciano, G. Raman analysis of tear fluid alteration following contact lense use. *Sensors (Basel)* **19**(15). https://doi.org/10.3390/s19153392 (2019).
30. Choi, S., Moon, S. W., Shin, J. H., Park, H. K. & Jin, K. H. Label-free biochemical analytic method for the early detection of adenoviral conjunctivitis using human tear biofluids. *Anal. Chem.* **86**(22), 11093–11099. https://doi.org/10.1021/ac5025478 (2014).
31. Steyerberg, E. W. & Harrell, F. E. Prediction models need appropriate internal, internal-external, and external validation. *J. Clin. Epidemiol.* **69**, 245–247. https://doi.org/10.1016/j.jclinepi.2015.04.005 (2015).

Acknowledgements

We would like to acknowledge the use of BioRender for the creation of the illustrations included in this paper. The visualizations significantly enhanced the clarity and presentation of our findings.

Author contributions

Y.B. W.: Conceptualization, Methodology, Writing - Original Draft. Y.L. H.: Investigation, Validation. X.B. L.: Investigation, Software, Formal analysis. C.S. K.: Investigation, Visualization. W.J. W.: Resources, Supervision, Writing - Review & Editing, Funding acquisition.

Funding

This work was supported by Natural Science Foundation of Fujian Province [grant number 2022J01121889] and Medical Innovation Project of Fujian Province [grant number 2023CXA001].

Declarations

Competing interests
The authors declare no competing interests.

Ethics approval
The Institutional Animal Care and Use Committee of Fujian Provincial Hospital approved all procedures involving animals (IACUC-FPH-SL-20230911[0093]). This study was performed in accordance with relevant guidelines and regulations. All methods are reported in accordance with ARRIVE guidelines.

Additional information
Supplementary Information The online version contains supplementary material available at https://doi.org/10.1038/s41598-025-85451-y.

Correspondence and requests for materials should be addressed to W.W.

Reprints and permissions information is available at www.nature.com/reprints.

Publisher's note Springer Nature remains neutral with regard to jurisdictional claims in published maps and institutional affiliations.